

KOTO: Search for Direct CP Violating $K_L \rightarrow \pi^0 \nu \bar{\nu}$ Decays

Yee B. Hsiung^{a,*} for the KOTO Collaboration

^a*Department of Physics, National Taiwan University,
1, Sec. 4, Roosevelt Rd., Taipei, Taiwan 10617*

E-mail: yhsprung@phys.ntu.edu.tw

We review the current status of JPARC KOTO experiment to search for very rare K_L decays to $\pi^0 \nu \bar{\nu}$ which is a FCNC and direct CP violating decay mode. KOTO has collected K_L decay data with 30 GeV high intensity proton beam on target at JPARC since 2015 with an increasing beam power yearly over this period up to 64.5 kW. The results from 2016-2018 dataset published in 2021 ($BR < 4.9 \times 10^{-9}$) revealed three candidate events in the signal region with 1.22 ± 0.26 estimated background events, which is dominated by the contamination of upstream charged kaon decays and was verified in a dedicated 2020 run after installing upstream charged beam veto. More physics data have been accumulated since then. The status of blind analysis and background reductions is presented in this report with future beam power projections at JPARC as well as KOTO-DAQ upgrades. Plans for KOTO-II upgrades beyond the Standard Model sensitivity (3×10^{-11}) are also discussed.

*21st Conference on Flavor Physics and CP Violation (FPCP 2023)
29 May - 2 June 2023
Lyon, France*

*Speaker

1. Introduction

The JPARC KOTO experiment is dedicated to search for the flavor changing neutral current (FCNC) decays, the direct CP -violating $K_L^0 \rightarrow \pi^0 \nu \bar{\nu}$ decay mode [1][2]. The branching ratio of $K_L^0 \rightarrow \pi^0 \nu \bar{\nu}$ is highly suppressed in the Standard Model (SM) calculation and is predicted to be $(3.00 \pm 0.30) \times 10^{-11}$ [3] with only two percent uncertainty. Therefore, measuring $K_L^0 \rightarrow \pi^0 \nu \bar{\nu}$ offers a stringent test of the SM (e.g. direct measurement of the height of unitarity triangle η in the CKM matrix) with a possibility discovering new FCNC physics beyond SM [4][5]. Despite the rareness of $K_L^0 \rightarrow \pi^0 \nu \bar{\nu}$ posing a hurdle to its measurement, KOTO has an excellent potential to probe this decay with an unprecedented sensitivity, based on the utilization of the high-intensity proton beam at J-PARC and the design of the hermetic veto system in its detector. So far, KOTO has improved the upper limit in $BR(K_L^0 \rightarrow \pi^0 \nu \bar{\nu})$ by approximately an order of magnitude at 3.0×10^{-9} [6], compared to the results from the previous experiments. In the coming years, KOTO is anticipated to improve the sensitivity of this measurement by another order of magnitude to below $O(10^{-10})$. In this article, we provide an overview of the recent results on the $K_L^0 \rightarrow \pi^0 \nu \bar{\nu}$ study from KOTO. Additionally, we outline the current status of the ongoing blind analysis using the data collected during 2019–2021 as well as upgrades on KOTO-DAQ to accommodate the future beam power projection at JPARC and newly installed upstream charged beam veto (UCV) detector for background suppression from the beam. Plans for KOTO-II upgrades beyond the Standard Model sensitivity (3×10^{-11}) are also discussed.

2. The KOTO Detector

The KOTO detector is a hermetic detector system that completely encloses the fiducial decay volume of incident neutral kaon particles, ensuring no particles of decay product go undetected. Figure 1 shows the cross sectional view of the KOTO detector. The CsI calorimeter is used to identify the $K_L^0 \rightarrow \pi^0 \nu \bar{\nu}$ decay by detecting the two photons from $\pi^0 \rightarrow \gamma\gamma$ via electromagnetic shower [7]. It consists of 2716 undoped CsI crystals, each has 50 cm in length (about 27 radiation length), covering a circular area with a radius of 90 cm centered along the beam axis with a 15×15 cm² beam hole at the end of decay region. The other detector components are used as vetoes to identify

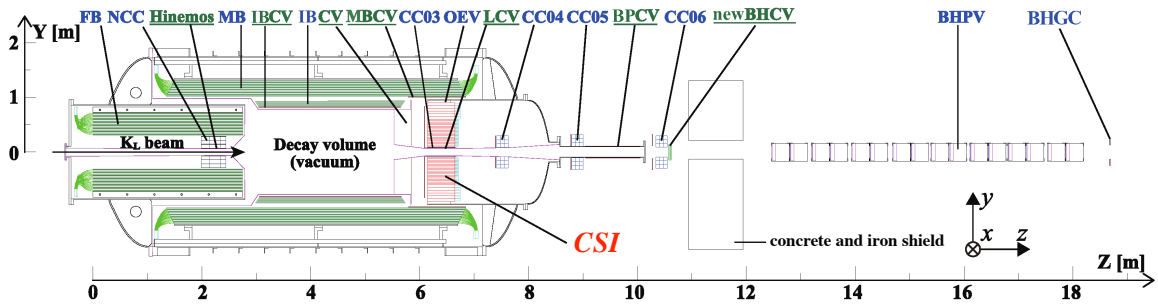


Figure 1: Cross sectional view of the KOTO detector. The beam enters from the left into the vacuum decay region. Detector components labeled in blue with their abbreviated names represent photon veto counters, and those labeled in green and underlined represent charged-particle veto counters. CSI is the main CsI calorimeter for detecting photons located at the end of decay region.

particles escaped from the CsI calorimeter detection. The Main Barrel (MB), Inner Barrel (IB), and Front Barrel (FB) detectors are the largest components in the veto system, covering the remaining areas of the fiducial decay volume in a cylindrical configuration. The NCC, CC03, CC04, CC05, and CC06 detectors are positioned along the beamline, forming a series of “collar” style vetoes of the beam line to detect particles escaping in the beam direction. Additionally, charged veto detectors are placed in front of the CsI (CV), the innermost layer of IB (IBCV), and along the beam pipe (LCV, BPCV). Furthermore, BHPV and BHCV detectors are placed within the downstream beamline after CsI calorimeter to detect in-beam photons and charged particles, respectively. The waveform from the detectors is recorded by either 125-MHz or 500-MHz sampling ADCs so that the pulse shape and timing information can be used in the analysis for the background rejection. Details of the apparatus are available in [6].

The neutral kaon beam is produced from a 66 mm-long gold target by a 30-GeV primary proton beam hitting the target at an angle of 16° to the K_L beamline through two collimators and a sweeping magnet between them [8] to sweep out the secondary charged particles before entering the vacuum decay volume. The target is located about 21.5m upstream of the FB which was defined as the origin of the z -axis ($Z = 0$). At the end of downstream collimator, the size of the neutral beam is $8 \times 8 \text{ cm}^2$ and the K_L flux is $2.1 \times 10^{-7} K_L$ s per incident proton on target with a peak K_L momentum 1.4 GeV/ c .

The deposited energy in adjacent CsI crystals of CSI are grouped into a cluster and used to reconstruct the photon energy, timing, and position. The opening angle between two photons is calculated by assuming they come from a π^0 with the nominal π^0 mass and decay along the beam axis. Therefore the π^0 decay vertex position (Z_{vtx}) and the π^0 four momentum can be calculated. Since the π^0 from $K_L^0 \rightarrow \pi^0 \nu \bar{\nu}$ decays is expected to have a finite transverse momentum (P_t) due to the missing neutrinos. Therefore we use the P_t vs Z_{vtx} plane to search for the candidate $K_L^0 \rightarrow \pi^0 \nu \bar{\nu}$ events in the decay volume.

3. Data Collection Periods and Previous Results

3.1 Datasets

The KOTO experiment at JPARC has conducted four periods of data collection since 2013, as shown in Figure 2. The accumulated protons on target are shown on the left axis and the proton beam power (kW) in red is shown on the right axis over the operation performance of JPARC accelerator in Figure 2. In 2021 JPARC achieved the highest 64.5 kW beam power before a one year shutdown for the accelerator beam upgrade. The effective statistics of data collected in these four data sets are translated into single event sensitivities (SES), which is defined as

$$\text{SES} = \frac{1}{N_{K_L^0} \times \mathcal{A}_{\text{sig}}}, \quad (1)$$

where $N_{K_L^0}$ is the number of collected kaon particles in each data period, and \mathcal{A}_{sig} is the acceptance of $K_L^0 \rightarrow \pi^0 \nu \bar{\nu}$ events after imposing all selection criteria. The acceptance \mathcal{A}_{sig} for $K_L^0 \rightarrow \pi^0 \nu \bar{\nu}$ is evaluated using GEANT4-based Monte Carlo (MC) simulations. Accidental activity in the detectors was recorded during physics data taking and overlaid onto the MC events to correct the

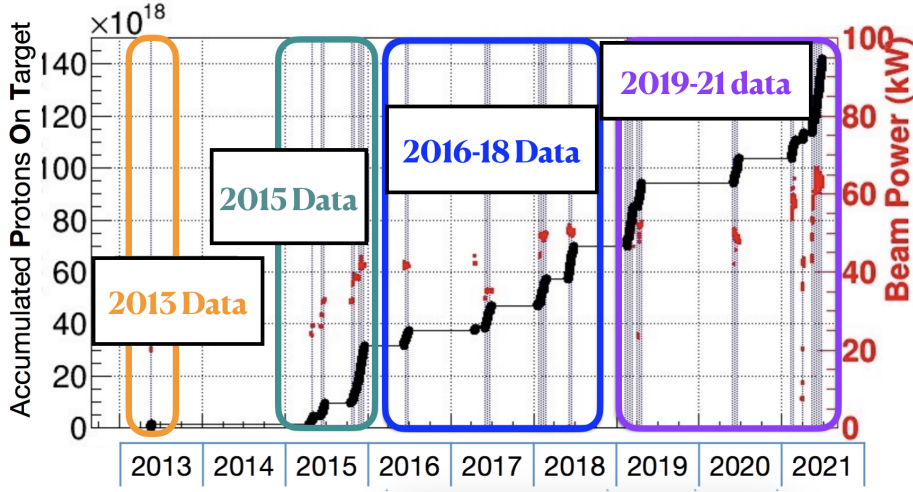


Figure 2: Accumulated protons on the target (left axis) in the past four data collection periods and the proton beam power (right axis) labeled in red from JPARC accelerator throughout the years.

beam intensity related event loss in acceptance. The SES is normalized with the $K_L^0 \rightarrow \pi^0 \pi^0$ decay sample which is collected in four-cluster trigger of CSI together with two-cluster physics trigger and corrected the background under the K_L mass peak to calculate the $\mathcal{N}_{K_L^0}$. The SES represents the branching ratio of $K_L^0 \rightarrow \pi^0 \nu \bar{\nu}$ for the detection of a single $K_L^0 \rightarrow \pi^0 \nu \bar{\nu}$ event within the statistics of a given dataset. The SES of each dataset collection period is summarized in Table 1.

Table 1: A summary of SESs of data collected in each data collection period.

Dataset	SES
2013	1.28×10^{-8}
2015	1.30×10^{-9}
2016-2018	7.2×10^{-10}
2019-2021	7.9×10^{-10} (2021 run only)

The analysis of the first three data sets (2013, 2015, 2016-2018) has been completed and published. The best upper limit in the measurement of $\text{BR}(K_L^0 \rightarrow \pi^0 \nu \bar{\nu})$ is an upper limit of 3.0×10^{-9} [6], which is based on the data collected in 2015 an order of magnitude improvement over 2013 dataset. The first physics run of KOTO was conducted in 2013 (after two years delay due to the 2011 Tohoku earthquake) with only 100 hours of data taking [9], but achieved a comparable sensitivity to previous E391a experiment at KEK [10], a substantial improvement in the proton beam power of JPARC. Recently released results are based on the data collected during 2016–2018 [11]. The analysis of 2019–2021 dataset is ongoing currently, and the results of 2021 run data are expected to be released later this year. Brief descriptions of the analysis results performed during these data periods are summarized in the sections below. Details of the analysis can be found in the published papers [6] and [11].

3.2 2015 Dataset

KOTO has collected data in 2015 corresponding to 2.2×10^{19} protons on target. In the 2015 dataset, no events were observed in the signal region of $K_L^0 \rightarrow \pi^0 \nu \bar{\nu}$, while the predicted number of background events was 0.42 ± 0.18 . With a SES of 1.3×10^{-9} , an upper limit on $\text{BR}(K_L^0 \rightarrow \pi^0 \nu \bar{\nu})$ was set to be 3.0×10^{-9} at the 90% confidence level (*C.L.*) [6]. This upper limit is the current world best limit for the measurement of $\text{BR}(K_L^0 \rightarrow \pi^0 \nu \bar{\nu})$. An upper limit for $K_L^0 \rightarrow \pi^0 X^0$ was also set as 2.4×10^{-9} , where X^0 is an invisible boson with a mass of $135 \text{ MeV}/c^2$, which improves the upper limit of direct search by almost an order of magnitude.

3.3 2016–2018 Dataset

The dataset collected during 2016–2018 (corresponding to 3.05×10^{19} protons on target) has an improved SES to be 7.2×10^{-10} with 9.2% uncertainty, which is approximately twice as good as the SES of the 2015 dataset. Within this dataset, three candidate events were observed in the signal region of $K_L^0 \rightarrow \pi^0 \nu \bar{\nu}$, with a predicted number of background events of 1.22 ± 0.26 [11], as shown in Figure 3. To avoid bias, the analysis was done with the blind analysis technique and a blind region in $\pi^0 P_t$ vs Z_{vtx} plane was pre-defined to be $120 < P_t < 260 \text{ MeV}/c$ and $2900 < Z_{\text{vtx}} < 5100 \text{ mm}$ as shown in Figure 3, where the signal region was defined as the area encompassing $120 < P_t < 250 \text{ MeV}/c$ and $3200 < Z_{\text{vtx}} < 5000 \text{ mm}$ excluding the area with $P_t < 1/35(Z_{\text{vtx}} - 4000 \text{ mm}) + 130 \text{ MeV}/c$ for $4000 < Z_{\text{vtx}} < 5000 \text{ mm}$ in order to suppress the background from $K_L^0 \rightarrow \pi^+ \pi^- \pi^0$ decays.

As described in [11] two newly discovered background sources arising from charged kaon decays and the beam-halo $K_L^0 \rightarrow \gamma\gamma$ decays were found and identified after examining the events in the blind region and additional background studies with MC.

The analysis was first proceeded according to the blind analysis procedure of 2015 data with improved background suppressions in the categories of known sources of K_L decays (such as $K_L^0 \rightarrow \pi^0 \pi^0 \pi^0$, $K_L^0 \rightarrow \pi^0 \pi^0$, etc.) and neutron induced background (such as hadronic clusters being misidentified as photon clusters in CSI, as well as $CV\text{-}\eta$ and $CV\text{-}\pi^0$ and upstream π^0 due to beam halo neutron hitting CV and upstream NCC to produce η and π^0 then decay to photons) in the blind region and surrounding control regions in Figure 3 with $Z_{\text{vtx}} > 2900 \text{ mm}$ and $0 < P_t < 500 \text{ MeV}/c$. The background was summarized in Table II in [11] and the background estimations were also described in the text. By summer of 2019, about 0.092 background events were estimated in the signal region from the above mentioned sources and no event observed in the control regions except the upstream region with $Z_{\text{vtx}} < 2900 \text{ mm}$. We then decided to unblind the analysis of the blind region to reveal the signal region for the Kaon2019 Conference in Perugia, Italy. However, after we unblind the analysis several candidate events were observed in the blind region as reported in the conference proceedings [12].

These two new dominant background sources are both from the upstream region of the KOTO detector. In the upstream region before the entrance of the KOTO detector, there are two sets of collimators serving the purpose of refining and aligning the neutral kaon beam. Both of the newly identified background sources originate from kaons scattering at the second collimator after the sweeping magnet located before the detector entrance. In the case of the charged kaon background, K^\pm particles are generated at the collimator surface and subsequently decay into $K^\pm \rightarrow \pi^0 e^\pm \nu$, with

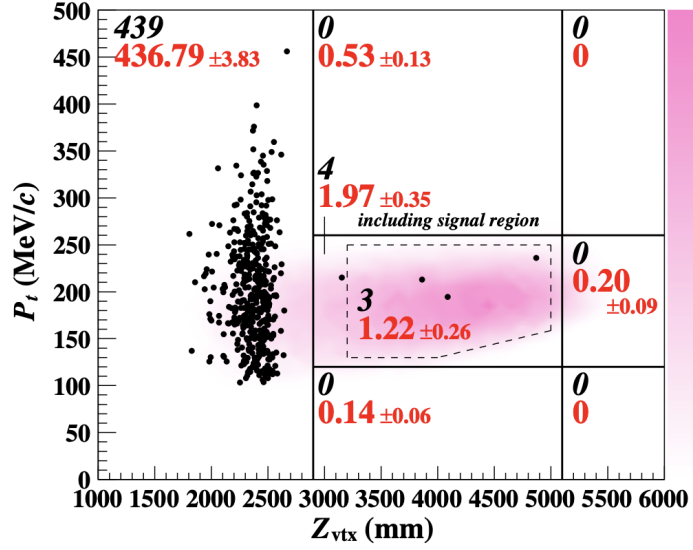


Figure 3: Reconstructed π^0 transverse momentum (P_t) versus decay vertex position (Z_{vtx}) of the 2016–2018 dataset with all the analysis cuts imposed. Three candidate events appeared in the signal region (surrounded by dotted lines) of $K_L^0 \rightarrow \pi^0 \nu \bar{\nu}$. The black dots represent observed events, and the shaded contour indicates the $K_L^0 \rightarrow \pi^0 \nu \bar{\nu}$ distribution from MC. The black italic (red regular) numbers are the number of observed (background) events for different regions. In particular, 1.22 ± 0.26 (1.97 ± 0.35) is the background expectation for the three (four) events observed inside the signal (blind) region.

the undetected e^\pm particles. The kinematics of the π^0 in the $K^\pm \rightarrow \pi^0 e^\pm \nu$ decay is similar to the one from the $K_L^0 \rightarrow \pi^0 \nu \bar{\nu}$ decay. The K^\pm flux at the beam exit was evaluated by using a $K^\pm \rightarrow \pi^0 \pi^\pm$ decay sample taken in a special run in 2020 with a dedicated trigger ($\pi^0 \pi^\pm$ trigger), which selected events with three clusters in CSI, one coincident hit in CV, and no coincident hits in other veto detectors. The ratio of the K^\pm to K_L flux at the beam exit was measured to be $(2.6 \pm 0.1) \times 10^{-5}$ and the K^\pm background was finally estimated to be 0.87 ± 0.25 after taking into account of the uncertainty of K^\pm spectrum and statistical uncertainty of the flux measurement.

On the other hand, the beam-halo $K_L^0 \rightarrow \gamma\gamma$ background occurs when the scattered kaon decays into $K_L^0 \rightarrow \gamma\gamma$, resulting the decayed photons possess large transverse momentum similar to the photons originating from $K_L^0 \rightarrow \pi^0 \nu \bar{\nu}$. The yield of the beam-halo K_L was evaluated by using $K_L^0 \rightarrow \pi^0 \pi^0 \pi^0$ events with large values of the radius position of the center of deposited energy (R_{COE}) in CSI, and the MC expectations. The number of the beam-halo $K_L^0 \rightarrow \gamma\gamma$ background events was estimated to be 0.26 ± 0.07 . With the two new background sources and the estimated total number of background events, 1.22 ± 0.26 , the corresponding probability of observing three events is 13%. So the number of observed events is statistically consistent with the background expectation and the upper limit on the branching fraction of the $K_L^0 \rightarrow \pi^0 \nu \bar{\nu}$ decay can be calculated as 4.9×10^{-9} at the 90% *C.L.*

To suppress the background from K^\pm decays in the future datasets after 2020, we are preparing a new charged-particle veto counter (UCV) to be installed in the beam at the upstream edge of the KOTO detector. We have developed and installed a prototype UCV consisting of 1 mm^2 scintillation fibers in 2020 special run to check its performance. We are also planning to install a new sweeping

magnet at the beam exit to reduce the number of K^\pm s entering the KOTO detector. New cuts to extract the true incident angle of the photons based on the cluster energy, timing and cluster shape are also under development. We expect these improvements will further suppress these two backgrounds.

4. Analysis Progress of 2021 Run

4.1 2019–2021 Dataset

In the analysis of the 2019–2021 dataset, several improvements were made to suppress the charged kaon and beam-halo $K_L^0 \rightarrow \gamma\gamma$ background sources. The first improvement involved the upgrade of UCV which is installed between the second collimator and the entrance of the KOTO detector. The new UCV comprises low-mass scintillating fibers (0.5 mm²) designed to detect K^\pm particles in the kaon beam, as shown in Figure 4. We used the silicon photo-sensors (MPPC) to readout the scintillating fibers of UCV. The detector is also tilted by 25° angle to reduce the inefficiency. Through the validation of collected data in 2021, the UCV can highly suppress the dominant $K^\pm \rightarrow \pi^0 e^\pm \nu$ background events by a factor of 13 with 97% signal efficiency after we reduced the fiber thickness to 0.5 mm in 2021 run.

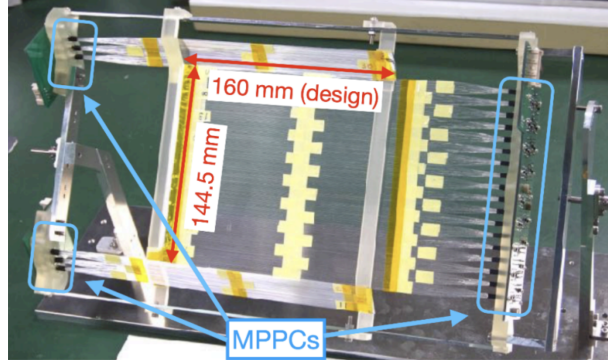


Figure 4: Picture of the new Upstream Charged Veto (UCV) detector. It comprises 0.5 mm thick scintillating fibers to detect charged kaon particles in the beam.

The second improvement is the development of an analysis technique for suppressing the beam-halo $K_L^0 \rightarrow \gamma\gamma$ background. This technique is based on the consistency between the incident angle of photons and the shapes of their clusters in the CsI calorimeter, as shown in Figure 5. In the case of a beam-halo $K_L^0 \rightarrow \gamma\gamma$ event, the true decay vertex of K_L^0 is displaced from the center of the beam axis due to the scattering process in the upstream (e.g. collimator surface). However, the reconstructed vertex is assumed to align with the beam axis. As a consequence, an inconsistency arises between the reconstructed incident angle of the photon and the observed cluster shapes in the CsI calorimeter. Therefore, we developed a likelihood ratio technique based on this phenomenon of multivariate analysis using Fisher Discriminant to separate the signal and background events. It effectively rejected the beam-halo $K_L^0 \rightarrow \gamma\gamma$ background by a factor of 15 while maintaining 90% signal efficiency of $K_L^0 \rightarrow \pi^0 \nu \bar{\nu}$ events in 2021 data.

Although the analysis of the 2019–2021 dataset is ongoing, a preliminary result of 2021 run shows that the predicted total number of background events in the extended signal region is reduced

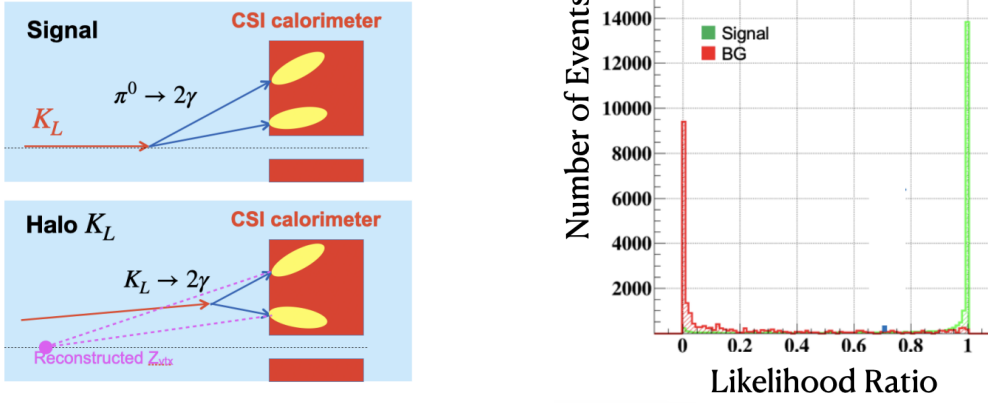


Figure 5: A drawing to explain the inconsistency between the photon angle and cluster shapes (left), and the result of a likelihood discrimination for suppressing the beam-halo $K_L^0 \rightarrow \gamma\gamma$ background events (right).

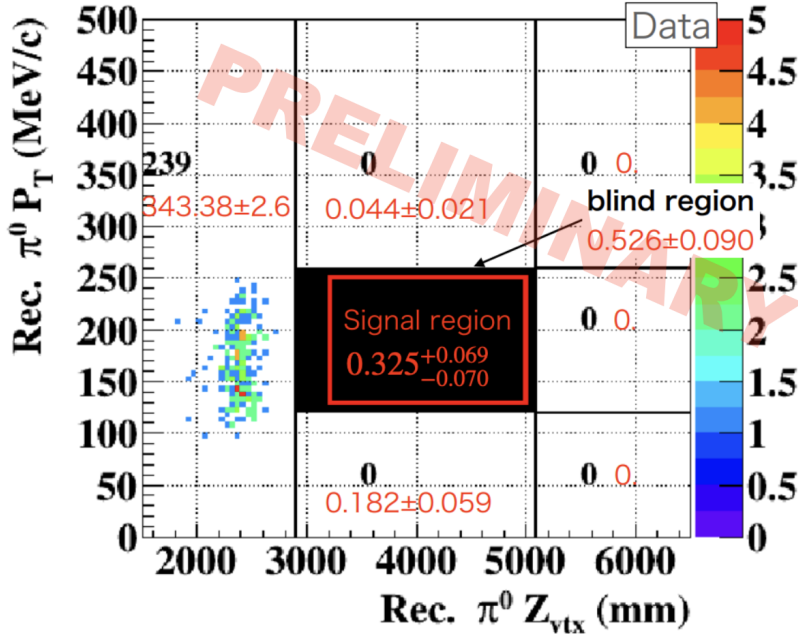


Figure 6: Preliminary plot of the reconstructed π^0 transverse momentum (P_T) versus decay vertex position (Z_{vtx}) of the 2021 data with all the analysis cuts imposed.

to 0.325 events, as shown in Figure 6 with a SES of 7.9×10^{-10} which is comparable to 2016-2018 dataset, due to higher proton beam power delivered by JPARC accelerator. Note that the background in blind region is also reduced to 0.526 events. The preliminary background estimation in the signal region is summarized in Table 2 with the current MC statistics from KEK computing clusters (KEKCC), where the improvement of the charged kaon background as well as the beam-halo and scattered $K_L^0 \rightarrow \gamma\gamma$ background are all reduced to the similar level of other backgrounds except the $K_L^0 \rightarrow \pi^0 \pi^0$ background which is now the dominant background to be 0.141 ± 0.059 .

We have investigated the change of $K_L^0 \rightarrow \pi^0 \pi^0$ background estimation between 2016-2018

Table 2: A summary of preliminary background estimation in signal region of 2021 data.

Source	Events in signal region
$K_L^0 \rightarrow \pi^0 \pi^0$	0.141 ± 0.059
K^\pm	$0.043 +0.016/-0.022$
Hadron cluster	0.042 ± 0.007
Beam-halo $K_L^0 \rightarrow \gamma\gamma$	0.013 ± 0.006
Scattered $K_L^0 \rightarrow \gamma\gamma$	0.025 ± 0.005
CV- η	0.023 ± 0.010
Upstream π^0	0.02 ± 0.02
$K_L^0 \rightarrow \pi^0 \pi^0 \pi^0$	0.019 ± 0.019
Total	$0.325 +0.069/-0.070$

dataset and 2021 data analysis. It is mainly due to change of GEANT4 version from v9.5.2 for 2016-2018 to v10.6.2 for 2021, in which the physics model of photonuclear (PN) reaction process was changed for better code management. Note that we see no difference between these two versions once we turn off the PN process in MC. As the result of background $K_L^0 \rightarrow \pi^0 \pi^0$ MC simulation from GEANT4 v10.6.2, the inefficiency of the barrel veto detectors at 1 MeV threshold has changed significantly due to PN reaction of photons at higher incident photon energy (e.g. increasing an order of magnitude at 400 MeV). Studies of 5γ data sample in CSI with one photon in barrel veto detectors at 1 MeV threshold to compare the inefficiency of barrel detectors for data and different version of GEANT4 MC. A discrepancy of photon veto inefficiency (about a factor of 2-3) appears between GEANT4 v9.5.2 and v10.6.2 at the level of 5×10^{-5} in data. More statistics of 5γ data sample in the future runs would be needed to confirm which GEANT4 version is correct. For now we will take a conservative approach for $K_L^0 \rightarrow \pi^0 \pi^0$ background estimation.

We plan to finalize the results of 2021 data later this year once we managed to increase the MC statistics by at least an order of magnitude by using the Open Science Grid (OSG) system for several background MC mass productions.

5. Upgrades and Current KOTO Status

In the near future for next three to four years, we expect an improvement in the sensitivity of the $K_L^0 \rightarrow \pi^0 \nu \bar{\nu}$ measurement by an order of magnitude, thanks to the JPARC beam intensity upgrade. This upgrade is completed in 2023 which will give an increase in beam power from 64.5 kW up to 80-100 kW. We have also made upgrades in KOTO DAQ system to increase the data taking rate from 10 k/spill to 25-30 k/spill via optical fibers from L1-FADCs to L2-OFCs and to 40 Gbps fiber switches to L3 spill nodes and disk nodes. Real time data transfer to KEKCC from KOTO L3 disk nodes has also been tested and installed. Upgrade of UCV with 0.2 mm thick scintillating fibers has also been prepared in 2023 with an installation of a new sweeping magnet downstream of the 2nd collimator. Assuming KOTO can secure 2-3 months of beam time for data taking in the coming years, we expect to collect 11 times more data by 2027, enabling us to improve the SES to below

$O(10^{-10})$, closing the gap to the SM $K_L^0 \rightarrow \pi^0 \nu \bar{\nu}$ prediction for the search of any new physics beyond the SM.

A new KOTO-II experiment for the Extended Hadron Experimental Facility upgrade at JPARC has been planned beyond 2027 with higher K_L flux and beam momentum by reducing the extraction angle to 5° of new K_L beamline. Longer decay volume and larger EM calorimeter for photon detection at the end of the decay region have been proposed and studied in MC. Options of photon detection for EM calorimeter and photon veto detectors along the barrel decay volume will also be studied in the near future with test beam of inefficiency measurements. The physics goal is to reach the SES to $O(10^{-13})$ with 40 SM $K_L^0 \rightarrow \pi^0 \nu \bar{\nu}$ signal events collected and a 1:1 signal to background ratio or better in several years of data taking runs.

References

- [1] L. S. Littenberg, *Phys. Rev. D* **39**, 3322 (1989).
- [2] V. Cirigliano, G. Ecker, H. Neufeld, A. Pich, and J. Portolés, *Rev. Mod. Phys.* **84**, 399 (2012), and references therein.
- [3] A. J. Buras, D. Buttazzo, J. Girrbach-Noe, and R. Knegjens, *J. High Energy Phys.* **1511**, 033 (2015).
- [4] X.-G. Xe, X.-D. Ma, J. Tandean, and G. Valencia, *J. High Energy Phys.* **2004**, 057 (2020).
- [5] J. Aebischer, A. J. Buras, and J. Kumar, *J. High Energy Phys.* **2012**, 097 (2020).
- [6] J. K. Ahn *et al.*, (KOTO Collaboration), *Phys. Rev. Lett.* **122**, 021802 (2019).
- [7] K. Sato *et al.*, *Nucl. Instrum. Methods A* **982**, 164527 (2020).
- [8] T. Shimogawa, *Nucl. Instrum. Methods A* **623**, 585 (2010).
- [9] J. K. Ahn *et al.* (KOTO Collaboration), *Prog. Theor. Exp. Phys.* **2017**, 021C01 (2017).
- [10] J. K. Ahn *et al.* (E391a Collaboration) *Phys. Rev. D* **81**, 072004 (2010).
- [11] J. K. Ahn *et al.*, (KOTO Collaboration), *Phys. Rev. Lett.* **126**, 121801 (2021).
- [12] S. Shinohara (on behalf of KOTO Collaboration), *J. Phys. Conf. Ser.* **1526**, 012002 (2020) in the proceedings of KAON2019, Perugia, Italy.